# ELECTRON BEAM LITHOGRAPHY PROCESS QUALITY IMPROVEMENT BY ROBUST ENGINEERING APPROACH

Lilyana Koleva[1], Asya Asenova-Robinzonova[1], Elena Koleva[1,2]

[1]*University of Chemical Technology and Metallurgy*
*8 Kliment Ohridski Blvd., Sofia 1797, Bulgaria*
[2]*Institute of Electronics, Bulgarian Academy of Sciences*
*72 Tzarigradsko Chaussee Blvd, 1784 Sofia, Bulgaria*
*E-mail: eligeorg@uctm.edu*

*Received 09 July 2023*
*Accepted 22 August 2023*
*DOI: 10.59957/jctm.v59.i2.2024.24*

## ABSTRACT

*The model-based robust approach is successfully applied to different industrial processes for improving their quality performance characteristics. The Robust engineering approach is implemented in cases of heteroscedasticity of the performance characteristics in presence of errors in the process parameters or noise factors, which is typical for the production processes. Higher quality and reproducibility of the quality characteristics can be achieved both for existing production processes or for technological process design at the production planning and development stages.*

*In this paper the model-based robust engineering approach is implemented for the quality improvement of polymethyl methacrylate (PMMA) resist profiles, obtained by electron beam lithography process. Specific technological requirements concerning the developed profile structures, their variances (reproducibility) in production conditions and robustness toward the errors in the process parameters, are considered. Different multicriteria optimization approaches were applying and compared, aiming to simultaneously fulfil the requirements for the geometric characteristics of the positive resist PMMA.*

*Keywords: industrial process optimization, quality improvement, robust engineering, electron beam lithography.*

## INTRODUCTION

The robust engineering design approach for quality improvement can be applied both for existing production processes or for technological process design at the production planning and development stages. When a technology for the specific product production has to be developed the following stages have to be realized: system design, tolerance design and parameter design. The implementation of the model-based robust engineering design methodology, combined with the analytical or/and empirical model-based process simulation, can lead to answers to some essential questions: what are the technological requirements of the planned for production products, is the chosen equipment (system) applicable for the production of the product, what are the requirements for the quality performance characteristics of the product and their acceptable tolerances, and what are the optimal process parameter settings for the production of products with high and reproducible quality.

The Robust engineering approach is implemented in cases of heteroscedasticity of the performance characteristics in presence of errors in the process parameters or noise factors [1]. Typically, such are the conditions in all industrial processes. Consequently, the methodology can be successfully applied to different production processes for product production design or for improving product quality performance characteristics and their variability [2 - 4]. The Robust engineering approach is based on finding models for the mean value and the variance of the performance characteristics [1]. The model of the mean value of the performance characteristic is:

$$\tilde{y}(x) = E\,[y(z)] = \eta(x) + \theta^T E(g), \quad (1)$$

where $\eta(x)$ is a model of the performance characteristic, for example polynomial regression obtained by the Response Surface Methodology. The second term takes into account the bias caused by the errors transmitted from the process parameters $x$ to the performance characteristic $\tilde{y}(x)$, where $\theta^T$ is the vector of the coefficients in the regression model ($\eta(x) = \theta^T F$), $F$ is a matrix of known functions $f$ (regressors matrix) of the process parameters $x$, defined by the regression model and the experiments that are done, $g = h - f$, $h$ is the matrix of the regressors in the regression model $z$, considered as containing errors $e$ (for any process parameter - $z_i = x_i + e_i$) and $E(g)$ is the mathematical expectation of $g$.

The model for the variance is:

$$\tilde{s}^2 = E(\theta^T \psi \psi^T \theta) + \sigma_\varepsilon^2 = \theta^T \Psi \theta + \sigma_\varepsilon^2, \quad (2)$$

where $\psi = g - E(g)$, is defined on the basis of the variances for each process parameters $x$, which can be calculated using the tolerance limits of the process parameters, $\Psi = E(\psi\psi^T)$ depends on the structure of the regression model and the experimental design, $\sigma_\varepsilon^2$ is the random error of the performance characteristic.

Electron beam lithography (EBL) is a key technology for the fabrication new generation integral circuits and devices of electronics, photonics and nowadays and future nanoengineering [5]. The EBL process of receiving a resist structure by electron beam exposure (stage 3) and development (stage 5) is visualized in Fig. 1 for the case of a positive electron resist (Polymethyl methacrylate - PMMA). Typical developers are methyl isobutyl ketone (MIBK), MIBK diluted with isopropanol alcohol (IPA) (1:1, 1:2 or 1:3) [6, 7].

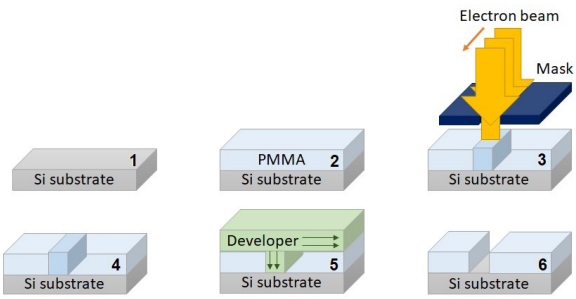


Fig. 1. Electron beam lithography - positive electron resist.

The computer simulation of the processes of electron exposure and development of the resist profile in EBL are important for the optimization of this expensive technological process, due to the use of most expensive technology equipment in the microelectronic fabrication, to the use of sophisticated materials and a long chain of sequential technology steps for obtaining of the desired micro- and nano-structures.

In this paper the model-based robust engineering approach is implemented for the quality improvement of the PMMA resist profiles obtained by EBL process. Specific technological requirements concerning the developed profile structures, their variances (reproducibility) in production conditions and robustness toward the errors in the process parameters, are considered. For the implementation of this methodology, two models for each of the output product characteristics are estimated - for their mean values and their variances. For the parameter optimization aiming the improvement of the quality performance characteristics according to pre-set technological requirements multicriteria robust optimization approaches are applied and compared.

## EXPERIMENTAL

An investigation of EBL process is performed based on numerical experiments with the simulation tool SELID [8]. As an example, it is chosen the exposure and the development of a layout with five parallel lines with 0.3 μm width, situated on 0.4 μm from each other (Fig. 2), and profile dimensions (Fig. 3) developed in a positive resist Polymethyl methacrylate (PMMA) central line. The measured performance characteristics are: (i) the measured width at a height of 55 % of the initial resist thickness ($d_0$) from the Si substrate - $y_1$ , μm, (ii) the measured width at a height of 5 % of the initial resist thickness ($d_0$) from the Si substrate - $y_2$, μm, (iii) width at the bottom - $y_3$, μm, - developed resist width at the interface PMMA resist - Si substrate, (iv) the average sidewall angle of the developed resist profile channel – $y_4$, °, – the average of the right $y_4^1$ and the left $y_4^2$ sidewall angles, measured between heights of 5 % and 90 % with respect to the initial resist thickness from the substrate, (iv) the thickness loss – $y_5$, %, measured as a percent with respect to the nominal resist thickness $d_0$.

In Fig. 3 the width $d_b$ is represented the width of the aperture (transparent zone) of the mask, used for

regulation of the irradiated by the electron beam zone. Due to the scattering of the penetrating into the resist and afterwards into the substrate electrons, as well as their backscattering from the substrate (proximity effect [9]) and due to the surface character of the development of the exposed latent image, the developed profile sizes does not coincide with the area from the resist surface, irradiated by electrons (mask width $d_b$). The chosen microstructure layout allows the study of 2D resist profiles, as shown in Fig. 3. The experimental conditions of numerical experiments done with the help of SELID computer simulating program are given in Table 1.

The influence of the variation EBL process parameters electron energy [keV], resist thickness [μm], development time [s], exposure dose [μC cm$^{-2}$] are investigated. 24 simulated experiments were realized, representing an optimal composite design for 4 factors. The experimental regions for the process parameter variation are presented in Table 2. Some of the obtained simulation results for the PMMA resist profiles are presented in Figs. 4 - 6.

From the presented Figs. 4 - 6 it is seen that the PMMA resist profile is strongly influenced by the EBL process parameters. The choice of optimal parameters is needed for obtaining nano-structures with good and repeatable quality, including the production of close to parallel resist profile sidewalls.

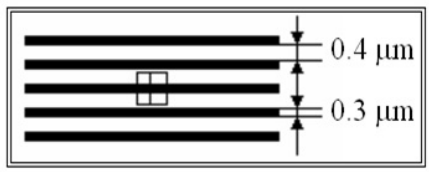


Fig. 2. Layout for PMMA resist exposure.

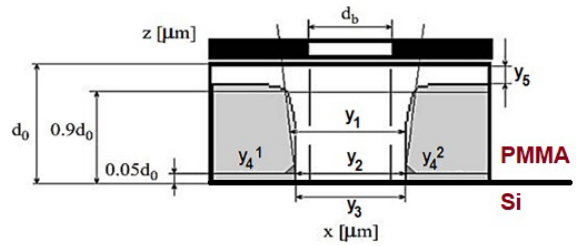


Fig. 3. Cross-section of the developed resist profile.

Table 1. The conditions at which the experiments are done with SELID simulation tool.

| | | |
|---|---|---|
| Exposure Parameters | Exposure Dose - [μC cm$^{-2}$] | $\tilde{p}_4$ |
| | Electron energy - [keV] | $\tilde{p}_1$ |
| | Spot shape - square, spot size [μm] | 0.02 |
| Wafer Parameters | Resist thickness - [μm] | $\tilde{p}_2$ |
| | PMMA | |
| | Mean atomic number | 3.6 |
| | Mean atomic weight [g mol$^{-1}$] | 6.66 |
| | Density [g cm$^{-1}$] | 1.2 |
| | Model | Pos_Dev |
| | Radiation Yield | 0.002 |
| | Resist | positive |
| | Substrate | SILICON |
| | Mean atomic number | 14 |
| | Mean atomic weight [g mol$^{-1}$] | 28.085 |
| | Density [g cm$^{-1}$] | 2.33 |
| Post-Exposure Bake | Diffusion Length [μm] | 0.01 |
| Development parameters | Time [s] | $\tilde{p}_3$ |
| Resolution [μm] | X and Y | 0.02 |
| | Z | 0.025 |

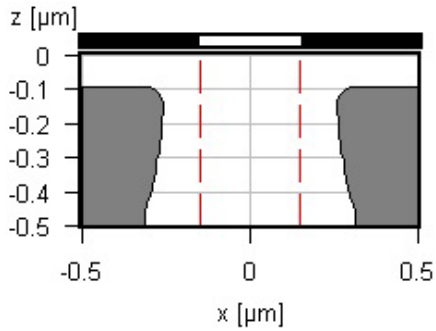


Fig. 4. 2D resist profile, obtained at electron energy 20 keV, resist thickness - 0.5 μm, development time - 360 s, exposure dose - 1300 μC cm$^{-2}$.

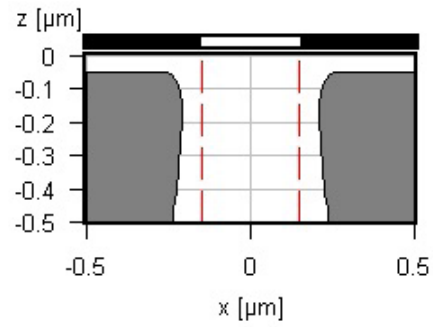


Fig. 5. 2D resist profile, obtained at electron energy 24 keV, resist thickness - 0.5 μm, development time - 240 s, exposure dose - 1300 μC cm$^{-2}$.

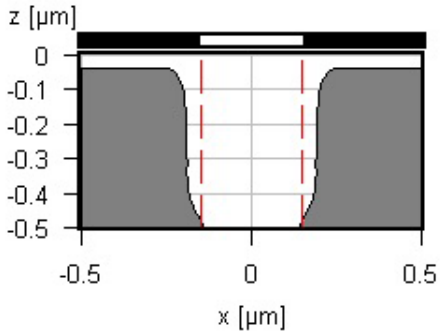


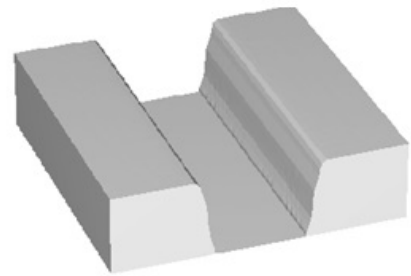

Fig. 6. 2D (a) and 3D (b) resist profile, obtained at electron energy 24 keV, resist thickness - 0.5 μm, development time - 240 s, exposure dose - 900 μC cm$^{-2}$.

Table 2. EBL investigation parameter ranges.

| Process parameter | Designation, coded | Minimum, $\tilde{p}_{min}$ | Base level, $\tilde{p}_0$ | Maximum, $\tilde{p}_{max}$ | Variation interval, λ |
|---|---|---|---|---|---|
| Electron energy [keV] | $p_1$ | 20 | 22 | 24 | 2 |
| Resist thickness [μm] | $p_2$ | 0.3 | 0.4 | 0.5 | 0.1 |
| Development time [s] | $p_3$ | 240 | 300 | 360 | 60 |
| Exposure dose [μC cm$^{-2}$] | $p_4$ | 900 | 1100 | 1300 | 200 |

## RESULTS AND DISCUSSION

### Robust model-based approach

The performed simulated experiments are used for estimation of regression models, describing the influence of the EBL process parameters: $\tilde{p}_1$ electron energy, keV, $\tilde{p}_2$ resist thickness, μm, $\tilde{p}_3$ development time, s, $\tilde{p}_4$ exposure dose, μC cm$^{-2}$, on the output quality characteristics. The regression models are estimated for process parameters in coded in the region [-1 ÷ 1] units. The relation between coded ($p_i$) and natural ($\tilde{p}_i$) units can be expressed by the equation:

$$p_i = (\tilde{p}_i - \tilde{p}_{0i})/\lambda_i \quad (3)$$

where $\tilde{p}_{0i}$ and $\lambda_i$ are the basic level and the interval of variation of each of the investigated process parameters (Table 2). In Table 3 are presented the estimated regression models, together with the determination coefficients, for (Fig. 3): $\hat{y}_1$, μm, - the width at a height of 55 % of the initial resist thickness, $\hat{y}_2$, μm - the width at a height of 5 % of the initial resist thickness, $\hat{y}_3$, μm, width at the bottom, $\hat{y}_4$, ° - the average sidewall angle of the developed resist profile channel,$\hat{y}_5$, % - the thickness loss.

The variation of the process parameters in production conditions can be estimated by their tolerance intervals.

Table 3. Regression models for the quality characteristics of the PMMA resist profiles, obtained by EBL.

| Regression model | $R^2$, % | $R^2_{adj}$, % |
|---|---|---|
| $\hat{y}_1 = 0.4557757 - 0.01838889p_1 + 0.03325253p_3 + 0.02452525p_4 + 0.00380841p_3p_4 - 0.0029375p_1p_3$ | 98.956 | 98.666 |
| $\hat{y}_2 = 0.47412699 - 0.02694444p_1 + 0.01305482p_2 + 0.04182612p_3 + 0.03199301p_4 - 0.007875p_1p_2 + 0.00879917p_2p_3 + 0.0076355p_2p_4 - 0.0059895p_2p_3p_4$ | 98.035 | 96.988 |
| $\hat{y}_3 = 0.48568848 - 0.03244444p_1 + 0.01455762p_2 + 0.04892645p_3 + 0.03775404p_4 - 0.01075p_1p_2 + 0.01480629p_2p_3 + 0.01238054p_2p_4 - 0.01024446p_2p_3p_4$ | 95.362 | 92.889 |
| $\hat{y}_4 = 95.905 - 2.2433333p_1 + 1.6697343p_2 + 1.7374913p_3 + 1.7243059p_4 - 1.558653p_3p_3 + 0.904375p_1p_3 + 1.4720837p_2p_3 - 1.2247872p_3p_4 + 0.899375p_1p_4 + 0.93971598p_2p_4 - 0.68903402p_2p_3p_4$ | 94.822 | 90.075 |
| $\hat{y}_5 = 14.935831 - 1.3444444p_1 - 3.5952283p_2 + 3.0161596p_3 + 2.1394548p_4 + 0.37634648p_1p_1 + 1.1988p_2p_2 + 0.28125p_1p_2 - 1.0515222p_2p_3 + 0.50713554p_3p_4 - 0.30625p_1p_3 - 0.45625p_1p_4 - 0.73986389p_2p_4 - 1.0735217p_1p_1p_2 + 0.62759036p_1p_1p_3 - 0.16486389p_2p_3p_4$ | 99.949 | 99.852 |

The used tolerance intervals of the input parameters are shown in Table 4.

The presented tolerance intervals are applied for estimation of the models for the mean values and variances of the studied quality characteristics under production conditions in order to consider the influence of the errors in the factor levels. Figs. 6 - 10 present the estimated models for the mean and the variance of each quality characteristic visualization by contour plots. All plots show the influence of the electron energy $\tilde{p}_1$ and the exposure dose $\tilde{p}_4$ for chosen constant values of the resist thickness $\tilde{p}_2$ = 0.4 μm and the development time $\tilde{p}_3$ = 300 s.

In Figs. 7 - 9 the mean widths between the sidewalls at different heights from the Si substrate surface, together with their variances are presented. It can be seen for all investigated mean widths that the increase of the electron energy leads to a decrease of the corresponding width, while the increase of the exposure dose leads to an increase of the widths. It is also seen that the resist profiles with higher widths correspond to higher values of the variances. Consequently, the smaller the width is, the better is its reproducibility for the considered process parameter conditions.

Fig. 10 presents contour plots of the mean $\tilde{y}_4$ and the variance $\tilde{\sigma}^2_4$ of the mean sidewall angle $y_4$ as a function from the electron energy $\tilde{p}_1$ and the exposure dose $\tilde{p}_4$ for a resist thickness $\tilde{p}_2$ = 0.4 μm and development time $\tilde{p}_3$ = 300 s. It can be observed that the increase of the electron energy reduces the mean sidewall angle, while the increase of the exposure dose increases the mean angle value. Since the obtaining parallel sidewalls is set as a target, and the contour lines close to 90° give good regimes for EBL process. The variance of the mean sidewall angle is largest for the smallest values of the angles (around 87°).

Table 4. Process parameters tolerance limits.

| Process parameter | Designation, coded | Tolerance limits |
|---|---|---|
| Electron energy [keV] | $p_1$ | $\tilde{p}_1 \pm 3\%\ \tilde{p}_1$ |
| Resist thickness [μm] | $p_2$ | $\tilde{p}_2 \pm 5$ |
| Development time [s] | $p_3$ | $\tilde{p}_3 \pm 5$ |
| Exposure dose [μC cm$^{-2}$] | $p_4$ | $\tilde{p}_4 \pm 10$ |

Contour plots of the mean $\tilde{y}_5$ and the variance $\tilde{\sigma}^2_5$ of the thickness loss $y_5$ % as a function from the electron energy $\tilde{p}_1$ and the exposure dose $\tilde{p}_4$ for a resist thickness $\tilde{p}_2$ = 0.4 μm and development time $\tilde{p}_3$ = 300 s are shown in Fig. 11. The minimal values of the mean values of the thickness loss are obtained for the largest electron energies and the smallest exposure doses. The variances for these process conditions are also the smallest.

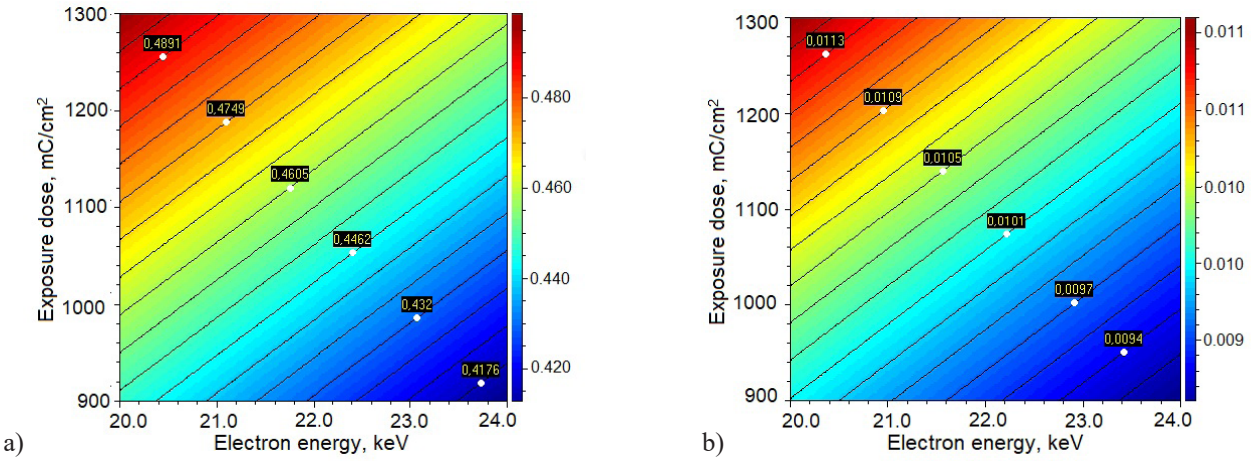


Fig. 7. Contour plots of the mean $\tilde{y}_1$ (a) and the variance $\tilde{\sigma}_1^2$ (b) of the width $y_1$ μm ($0.55d_0$) as a function from the electron energy $\tilde{p}_1$ and the exposure dose $\tilde{p}_4$ for a resist thickness $\tilde{p}_2$ = 0.4 μm and development time $\tilde{p}_3$ = 300 s.

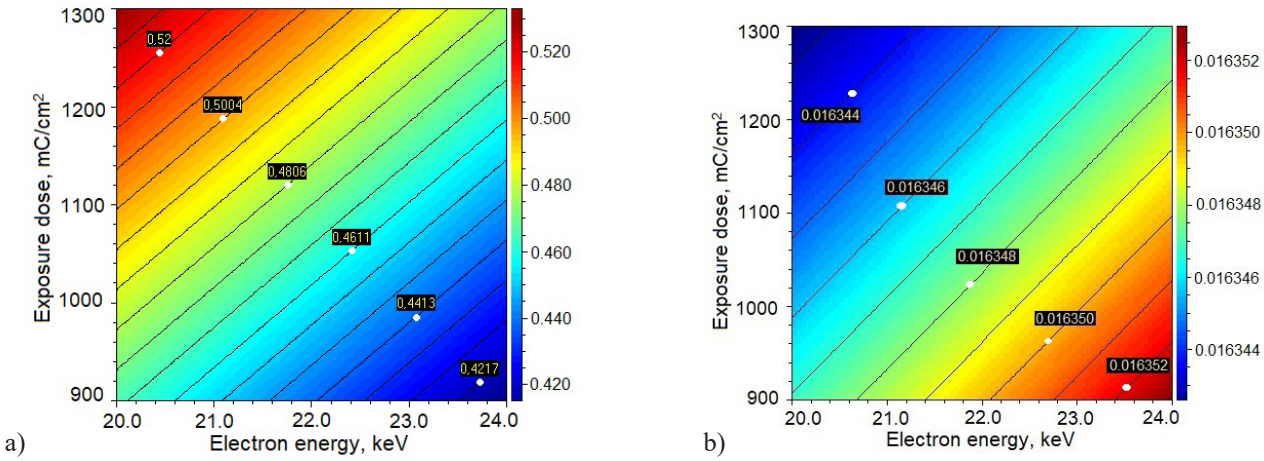


Fig. 8. Contour plots of the mean $\tilde{y}_2$ (a) and the variance $\tilde{\sigma}_2^2$ (b) of the width $y_2$ μm ($0.05d_0$) as a function from the electron energy $\tilde{p}_1$ and the exposure dose $\tilde{p}_4$ for a resist thickness $\tilde{p}_2$ = 0.4 μm and development time $\tilde{p}_3$ = 300 s.

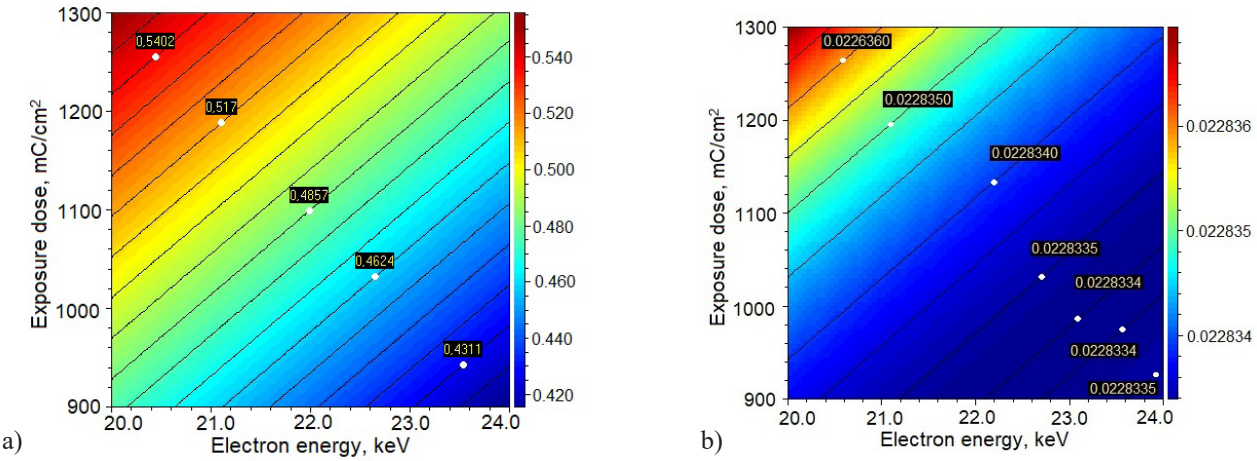


Fig. 9. Contour plots of the mean $\tilde{y}_3$ (a) and the variance $\tilde{\sigma}_3^2$ (b) of the width $y_3$ at the bottom μm as a function from the electron energy $\tilde{p}_1$ and the exposure dose $\tilde{p}_4$ for a resist thickness $\tilde{p}_2$ = 0.4 μm and development time $\tilde{p}_3$ = 300 s.

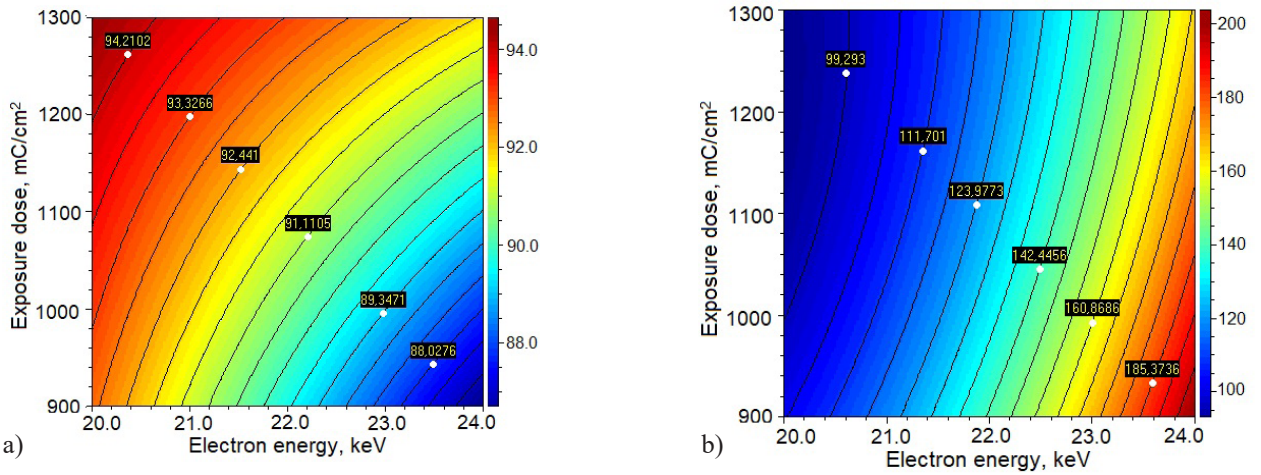


Fig. 10. Contour plots of the mean $\tilde{y}_4$ (a) and the variance $\tilde{\sigma}_4^2$ (b) of the mean sidewall angle $y_4$ as a function from the electron energy $\tilde{p}_1$ and the exposure dose $\tilde{p}_4$ for a resist thickness $\tilde{p}_2 = 0.4$ μm and development time $\tilde{p}_3 = 300$ s.

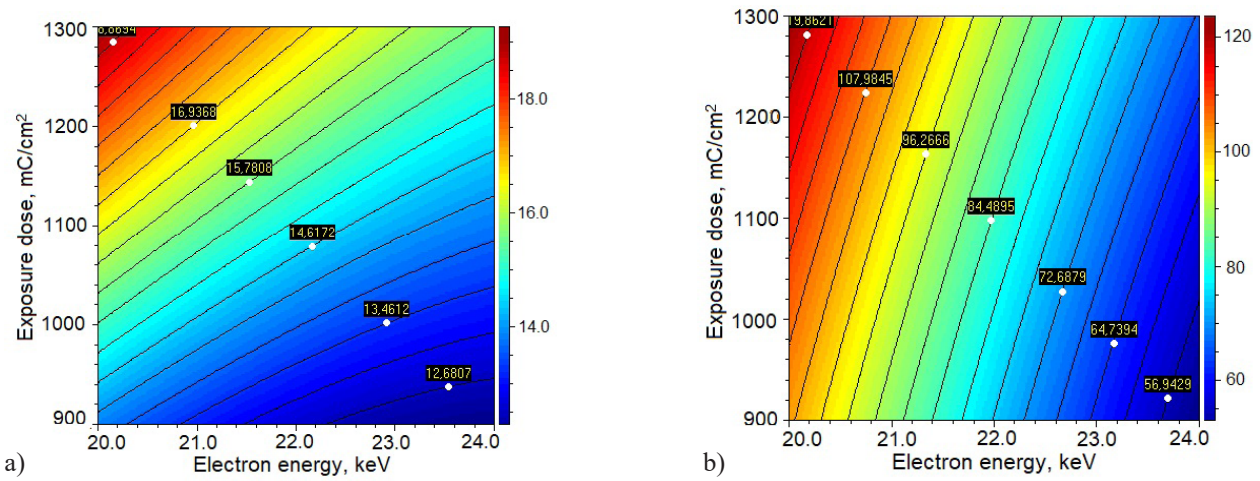


Fig. 11. Contour plots of the mean $\tilde{y}_5$ (a) and the variance $\tilde{\sigma}_5^2$ (b) of the thickness loss $y_5$% as a function from the electron energy $\tilde{p}_1$ and the exposure dose $\tilde{p}_4$ for a resist thickness $\tilde{p}_2 = 0.4$ μm and development time $\tilde{p}_3 = 300$ s.

**Multicriterial optimization**

During the production of resist structures, the goal is to achieve parallel walls of the cross-sections of the developed PMMA resist profiles with highest quality and reproducibility or minimum variation, caused by the errors in the factor levels. Choosing an appropriate optimization method is an important prerequisite for solving the optimization problems.

***Graphical optimization***

The technological constraints, related to the mean values of the widths of the cross-sections of the resist profiles at different heights - $\tilde{y}_1(p)$, $\tilde{y}_2(p)$, $\tilde{y}_3(p)$ and the mean angle of the sidewalls of the resists $\tilde{y}_4(p)$in production conditions, are set as:

- $0.395 \le \tilde{y}_1(p) \le 0.405$ μm,
- $0.395 \le \tilde{y}_2(p) \le 0.405$ μm,
- $0.395 \le \tilde{y}_3(p) \le 0.405$ μm,
- $83° \le \tilde{y}_4(p) \le 90°$.

Thus, the desired resist profiles will have structure width of 0.400 μm with tolerance of 0.005 μm and walls as close as possible to parallel in a large region of the sidewall structure.

The estimated robust models for the means are used for performing a graphical optimization of resist thickness loss - $\tilde{y}_5(p)$ depending on the variation of the electron energy - $\tilde{p}_1$ and exposure doses - $\tilde{p}_4$ for a resist thickness $\tilde{p}_2 = 0.4$ μm and exposure time $\tilde{p}_3 = 240$ s. In Fig. 12 the results from the graphical optimization for the process parameters the electron energy $\tilde{p}_1$ and the

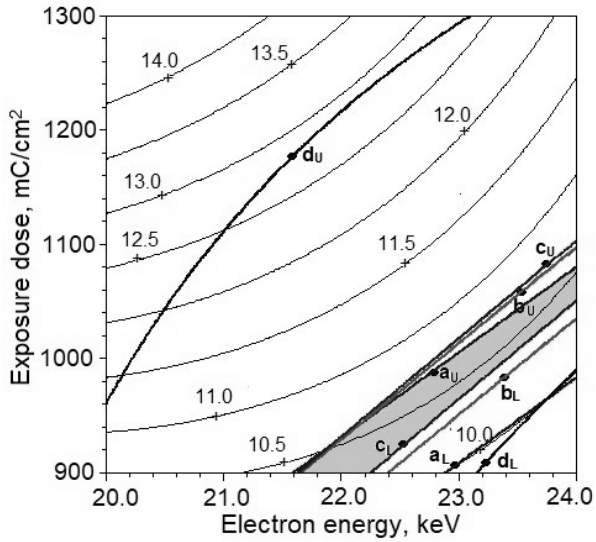


Fig. 12. Graphical optimization – resist thickness loss $\tilde{y}_5(p)$ as a function from the electron energy $\tilde{p}_1$ and the exposure dose $\tilde{p}_4$ for a resist thickness $\tilde{p}_2$ = 0.4 μm and development time $\tilde{p}_3$ = 240 s.

exposure dose $\tilde{p}_4$ are presented. The coloured region represents the region of these process parameters ($\tilde{p}_1$ and $\tilde{p}_4$), which result in resist profiles with heights - $\tilde{y}_1(p)$, $\tilde{y}_2(p)$, $\tilde{y}_3(p)$ and mean angle of the sidewalls of the resists $\tilde{y}_4(p)$ fulfilling all set constraints for constant values of the resist thickness $p_2$ and development time $p_3$. The constraints for different quality characteristics are signed as follows: $a_U$ - $\tilde{y}_1(p)$ = 0.405 μm, $a_L$ $\tilde{y}_1(p)$ = 0.395 μm, $b_U$ - $\tilde{y}_2(p)$ = 0.405 μm, $b_L$ - $\tilde{y}_2(p)$ = 0.395 μm, $c_U$ - $\tilde{y}_3(p)$ = 0.405 μm, $c_L$ $\tilde{y}_3(p)$ = 0.395 μm, $d_U$ - $\tilde{y}_4(p)$ = 90°, $d_L$ - $\tilde{y}_4(p)$ = 83°.

From Fig. 12 it can be seen that the PMMA resist thickness losses for the obtained optimal regimes will be between 10 % and 11 % from the initial resist thickness $\tilde{p}_2$ = 0.4 μm. The developed resist thickness after exposure and development will be between 0.356 and 0.360 μm. This also should be considered if it is critical for the nano-stricture functionality.

For the purposes of the study, a one-criteria optimization of the mean value of the thickness loss of the resist $\tilde{y}_5(p)$ and the set constraints on the mean values of the widths of the cross-sections of the profiles of the resists at different heights and of the angle of the sidewalls of the developed resists were carried out. The minimum value for the mean value of the resistance thickness loss - $\tilde{y}_{5,min}(p)$ = 9.52 % was obtained and at optimal values of the process parameters: $\tilde{p}_{1opt}$ = 24 keV, $\tilde{p}_{2opt}$ = 0.4342 μm, $\tilde{p}_{3opt}$ = 240.02 s and $\tilde{p}_{4opt}$ = 1075.6 μC cm$^{-2}$. The mean values of the other quality parameters are: $\tilde{y}_1(p)$ = 0.4046 μm, $\tilde{y}_2(p)$ = 0.3997 μm, $\tilde{y}_3(p)$ = 0.405 μm, $\tilde{y}_3(p)$= 0.3950 μm, $\tilde{y}_4(p)$ = 84.7°. The developed PMMA resist thickness in this case is expected to be equal to 0.393 μm.

### *Overall function strategies for multicriterial optimization*

In order to fulfil the multiple criteria requirements Pareto multicriterial optimization approach can be applied. Each Pareto-optimal solution makes some compromise toward some or all quality criteria to certain extend at the same time. If we compare randomly chosen two Pareto-optimal solutions some of the quality characteristics will have better values, but at least one will be worse.

The set multicriterial optimization requirements are presented in Table 5. The requirements should be fulfilled simultaneously, considering the quality parameter constraints.

Pareto-optimal compromise solutions are obtained (50 solutions) by applying genetic algorithm and the statistical software QstatLab [10]. In order to choose one solution from all we need additional analysis. This choice can be done by considering additional criteria (not included in the optimization task), by evaluation based on expert opinion or by definition of an overall function like loss function, desirability function, etc.

### *Optimistic strategy*

The *optimistic strategy* is based on the method of the function of losses. This optimization approach is called "optimistic" because the best possible values $q_j^{Opt}$ ($j$ = 1, 2, 3, …, $m$) are assigned to the reference (uncompromised) values of the quality characteristic $q_i(x)$. The reference values depend on the required minimum or maximum value for each of the quality characteristics. They are determined from the obtained Pareto-optimal solutions or in this case the differences between the best values and the optimistic reference values are minimized. The generalized function of losses $F^{Opt}(x)$ that has to be minimized is [11]:

$$F^{Opt}(x) = \frac{1}{m}\sum_{j=1}^{m}\left(\frac{q_j^{Opt} - q_j(x)}{\Delta_j}\right)^2 \quad (4)$$

$$\Delta j = q_{max,j} - q_{min,j} \quad (5)$$

Table 5. Requirements and constraints for the quality parameters.

| Requirements - means | Requirements - variances | Constraints |
|---|---|---|
| $\tilde{\bar{y}}_1 \rightarrow$ *maximum;* | $\tilde{\sigma}_1^2 \rightarrow$ *minimum;* | $0.395 \le \tilde{y}_1(p) \le 0.405$ μm, |
| $\tilde{\bar{y}}_2 \rightarrow$ *maximum;* | $\tilde{\sigma}_2^2 \rightarrow$ *minimum;* | $0.395 \le \tilde{y}_2(p) \le 0.405$ μm, |
| $\tilde{\bar{y}}_3 \rightarrow$ *maximum;* | $\tilde{\sigma}_3^2 \rightarrow$ *minimum;* | $0.395 \le \tilde{y}_3(p) \le 0.405$ μm, |
| $\tilde{\bar{y}}_4 \rightarrow$ *maximum;* | $\tilde{\sigma}_4^2 \rightarrow$ *minimum;* | $83° \le \tilde{y}_4(p) \le 90°$. |
| $\tilde{\bar{y}}_5 \rightarrow$ *minimum;* | $\tilde{\sigma}_5^2 \rightarrow$ *minimum;* | |

Table 6. Goals, reference values and the maximal and minimal characteristic values qj(x).

| Param. | $\tilde{y}_1(p)$ [μm] | $\tilde{y}_2(p)$ [μm] | $\tilde{y}_3(p)$ [μm] | $\tilde{y}_4(p)$ [°] | $\tilde{y}_5(p)$ [%] | $\tilde{s}_1^2(p)$ | $\tilde{s}_2^2(p)$ | $\tilde{s}_3^2(p)$ | $\tilde{s}_4^2(p)$ | $\tilde{s}_5^2(p)$ |
|---|---|---|---|---|---|---|---|---|---|---|
| Goal | max ↑ | max ↑ | max ↑ | max ↑ | min ↓ | min ↓ | min ↓ | min ↓ | min ↓ | min ↓ |
| $p_j^{Opt}$ | 0.4028 | 0.4025 | 0.4049 | 84.95 | 10.67 | 0.0075 | 0.0133 | 0.0176 | 253.5656 | 44.0624 |
| $p_j^{Pes}$ | 0.3952 | 0.3958 | 0.3951 | 83.76 | 13.85 | 0.0082 | 0.0159 | 0.0221 | 345.4103 | 65.8965 |
| $p_{j,max}$ | 0.4028 | 0.4025 | 0.4049 | 84.95 | 13.85 | 0.0082 | 0.0159 | 0.0221 | 345.4103 | 65.8965 |
| $p_{j,min}$ | 0.3952 | 0.3958 | 0.3951 | 83.76 | 10.67 | 0.0075 | 0.0133 | 0.0176 | 253.5656 | 44.0624 |
| $\Delta j$ | 0.0076 | 0.0067 | 0.0098 | 1.19 | 3.18 | 0.0007 | 0.0026 | 0.045 | 91.8447 | 21.8341 |

where $q_j(x)$ is the value for the *j-th* quality characteristic obtained at a given Pareto-optimal solution, $q_{max,j}$ and $q_{min,j}$ are the maximal and minimal values of each characteristic from all obtained 50 Pareto-optimal solutions and are presented in Table 6, together with calculated value for $\Delta_j$. Each reference value $q_j^{Opt}$ is obtained usually for different set of optimal process parameters $z_i$ and cannot be obtained simultaneously.

The best 5 optimal solutions obtained by implementation of the Optimistic method are presented in Table 7. They have smallest values of the function of losses $F^{opt}(x)$ from the arranged in ascending order results from all obtained 50 Pareto-optimal solutions. It can be seen that the best result is obtained for $F^{opt}(x) = 0.2063$, as well as the optimal values of the process parameters ($z_i$) at which it can be obtained in production conditions.

***Pessimistic strategy***

The pessimistic strategy is based on the function of usefulness method. In this strategy the worst possible (among the obtained Pareto-optimal solutions) or the "pessimistic" values $q_j^{Pes}$ ($j = 1, 2, 3, \ldots, m$) are assigned as reference values of the quality characteristic $q_i(x)$, again depending on the required minimum or maximum value for each quality characteristic from Pareto-optimal solutions. The function $F^{Pes}(x)$ that has to be maximized is [11]:

$$F^{Pes}(x) = \frac{1}{m}\sum_{j=1}^{m}\left(\frac{q_j(x) - q_j^{Pes}}{\Delta_j}\right)^2 \quad (6)$$

The best 5 optimal solutions obtained by implementation of the Pessimistic strategy are presented in Table 8. They have largest values of the function of usefulness $F^{Pes}(x)$ from the arranged in descending order results from all obtained 50 Pareto-optimal solutions.

***Bracketing approach for multi-criteria optimization***

The bracketing multi-criteria optimization strategy combines the optimistic and pessimistic approaches. Here the optimal compromise solution is searched by simultaneously minimizing the under-achievement to the best values (reference values) $q_j^{Opt}$ and maximizing the over-achievement over the required (worst) values $q_j^{Pes}$ [11].

The optimization function that has to be maximized in this case is:

$$F^{Br}(x) = \frac{1}{m}\sum_{j=1}^{m}\left(\frac{q_j(x) - q_j^{Pes}}{\Delta_j}\right)^2 - \frac{1}{m}\sum_{j=1}^{m}\left(\frac{q_j^{Opt} - q_j(x)}{\Delta_j}\right)^2 \quad (7)$$

The best 5 optimal solutions obtained by implementation of the Bracketing strategy are presented in Table 9. They have largest values of the function of

Table 7. Optimal solution by Optimistic strategy.

| № | $F^{opt}$ | $\tilde{p}_1$ | $\tilde{p}_2$ | $\tilde{p}_3$ | $\tilde{p}_4$ | $\tilde{y}_1(p)$ | $\tilde{y}_2(p)$ | $\tilde{y}_3(p)$ | $\tilde{y}_4(p)$ | $\tilde{y}_5(p)$ | $\tilde{s}_1^2(p)$ | $\tilde{s}_2^2(p)$ | $\tilde{s}_3^2(p)$ | $\tilde{s}_4^2(p)$ | $\tilde{s}_5^2(p)$ |
|---|---|---|---|---|---|---|---|---|---|---|---|---|---|---|---|
| 1 | 0.2063 | 24 | 0.349 | 246.648 | 1009.937 | 0.4009 | 0.3999 | 0.4025 | 84.2522 | 12.4098 | 0.0077 | 0.0145 | 0.0195 | 312.6974 | 55.2903 |
| 2 | 0.2161 | 24 | 0.365 | 242.623 | 1043.315 | 0.4025 | 0.4006 | 0.4016 | 84.3717 | 11.7282 | 0.0077 | 0.015 | 0.0204 | 326.4092 | 50.8654 |
| 3 | 0.2198 | 24 | 0.352 | 268.766 | 921.512 | 0.4015 | 0.4012 | 0.4035 | 84.7458 | 12.8059 | 0.0081 | 0.0146 | 0.0197 | 263.5504 | 58.1801 |
| 4 | 0.2234 | 24 | 0.363 | 242.994 | 1038.214 | 0.4021 | 0.4002 | 0.4014 | 84.326 | 11.7743 | 0.0077 | 0.015 | 0.0203 | 325.5278 | 51.1713 |
| 5 | 0.2308 | 24 | 0.340 | 262.120 | 936.302 | 0.4001 | 0.4004 | 0.404 | 84.4935 | 13.1144 | 0.008 | 0.0142 | 0.019 | 275.8632 | 60.3335 |

Table 8. Optimal solution by Pessimistic strategy.

| № | $F^{Pes}$ | $\tilde{p}_1$ | $\tilde{p}_2$ | $\tilde{p}_3$ | $\tilde{p}_4$ | $\tilde{y}_1(p)$ | $\tilde{y}_2(p)$ | $\tilde{y}_3(p)$ | $\tilde{y}_4(p)$ | $\tilde{y}_5(p)$ | $\tilde{s}_1^2(p)$ | $\tilde{s}_2^2(p)$ | $\tilde{s}_3^2(p)$ | $\tilde{s}_4^2(p)$ | $\tilde{s}_5^2(p)$ |
|---|---|---|---|---|---|---|---|---|---|---|---|---|---|---|---|
| 1 | 0.662421 | 24 | 0.3534 | 272.838 | 914.741 | 0.4025 | 0.4025 | 0.4048 | 84.9453 | 12.9181 | 0.0082 | 0.0146 | 0.0197 | 253.5656 | 58.9462 |
| 2 | 0.603062 | 24 | 0.3532 | 271.9969 | 913.321 | 0.402 | 0.4019 | 0.4041 | 84.8679 | 12.8687 | 0.0082 | 0.0146 | 0.0197 | 256.1519 | 58.682 |
| 3 | 0.592644 | 24 | 0.3501 | 271.588 | 912.047 | 0.4017 | 0.4017 | 0.4043 | 84.8291 | 12.9751 | 0.0082 | 0.0145 | 0.0195 | 256.4287 | 59.5074 |
| 4 | 0.572207 | 24 | 0.348 | 270.082 | 915.624 | 0.4014 | 0.4015 | 0.4043 | 84.774 | 13.017 | 0.0082 | 0.0144 | 0.0194 | 259.3267 | 59.7803 |
| 5 | 0.539228 | 24 | 0.3571 | 271.175 | 913.867 | 0.4017 | 0.4011 | 0.4029 | 84.808 | 12.6596 | 0.0082 | 0.0147 | 0.0199 | 259.8383 | 57.2057 |

Table 9. Optimal solution by Bracketing approach.

| № | $F^{br}$ | $\tilde{p}_1$ | $\tilde{p}_2$ | $\tilde{p}_3$ | $\tilde{p}_4$ | $\tilde{y}_1(p)$ | $\tilde{y}_2(p)$ | $\tilde{y}_3(p)$ | $\tilde{y}_4(p)$ | $\tilde{y}_5(p)$ | $\tilde{s}_1^2(p)$ | $\tilde{s}_2^2(p)$ | $\tilde{s}_3^2(p)$ | $\tilde{s}_4^2(p)$ | $\tilde{s}_5^2(p)$ |
|---|---|---|---|---|---|---|---|---|---|---|---|---|---|---|---|
| 1 | 3.88368 | 24 | 0.3534 | 272.838 | 914.741 | 0.4025 | 0.4025 | 0.4048 | 84.9453 | 12.9181 | 0.0082 | 0.0146 | 0.0197 | 253.5656 | 58.9462 |
| 2 | 3.34953 | 24 | 0.3532 | 271.997 | 913.321 | 0.402 | 0.4019 | 0.4041 | 84.8679 | 12.8687 | 0.0082 | 0.0146 | 0.0197 | 256.1519 | 58.682 |
| 3 | 3.018021 | 24 | 0.3501 | 271.588 | 912.047 | 0.4017 | 0.4017 | 0.4043 | 84.8291 | 12.9751 | 0.0082 | 0.0145 | 0.0195 | 256.4287 | 59.5074 |
| 4 | 2.936037 | 24 | 0.3571 | 271.175 | 913.867 | 0.4017 | 0.4011 | 0.4029 | 84.808 | 12.6596 | 0.0082 | 0.0147 | 0.0199 | 259.8383 | 57.2057 |
| 5 | 2.895932 | 24 | 0.3758 | 244.095 | 1039.504 | 0.4028 | 0.4002 | 0.4003 | 84.422 | 11.3563 | 0.0077 | 0.0154 | 0.0211 | 327.6867 | 48.2835 |

Table 10. Comparison of implemented optimization strategies.

| Param. | $\tilde{y}_1$(p) [μm] | $\tilde{y}_2$(p) [μm] | $\tilde{y}_3$(p) [μm] | $\tilde{y}_4$(p) [°] | $\tilde{y}_5$(p) [%] | $\tilde{s}_1^2(p)$ | $\tilde{s}_2^2(p)$ | $\tilde{s}_3^2(p)$ | $\tilde{s}_4^2(p)$ | $\tilde{s}_5^2(p)$ |
|---|---|---|---|---|---|---|---|---|---|---|
| Goal | max ↑ | max ↑ | max ↑ | max ↑ | min ↓ | min ↓ | min ↓ | min ↓ | min ↓ | min ↓ |
| $q_j^*$ | 0.4028 | 0.4025 | 0.4049 | 84.95 | 10.67 | 0.0075 | 0.0133 | 0.0176 | 253.5656 | 44.0624 |
| $\Delta j$ | 0.0076 | 0.0067 | 0.0098 | 1.19 | 3.18 | 0.0007 | 0.0026 | 0.045 | 91.8447 | 21.8341 |
| $q_{j,opt}$, *Opt* | 0.4009 | 0.3999 | 0.4025 | 84.25 | 12.41 | 0.0077 | 0.0145 | 0.0195 | 312.6974 | 55.2903 |
| $\delta_{oj}$ | 0.0019 | 0.0026 | 0.0024 | 0.69 | 1.74 | 0.0002 | 0.0012 | 0.0019 | 59.1318 | 11.2279 |
| $\delta_{rj}$,% | 25 | 38.806 | 24.4898 | 58.23 | 54.67 | 28.571 | 46.1538 | 4.2222 | 64.3824 | 51.4237 |
| $q_{j,opt}$, *Pes/Br* | 0.4025 | 0.4025 | 0.4048 | 84.95 | 12.92 | 0.0082 | 0.0146 | 0.0197 | 253.5656 | 58.9462 |
| $\delta_{oj}$ | 0.0003 | 0 | 0.00004 | 0 | 2.25 | 0.0007 | 0.0013 | 0.0021 | 0 | 14.8838 |
| $\delta_{rj}$,% | 3.9474 | 0 | 1.0204 | 0 | 70.65 | 100 | 50 | 4.6667 | 0 | 68.1677 |

usefulness $F^{Br}(x)$ from the arranged in descending order results from all obtained 50 Pareto-optimal solutions (their numbers are kept in the table). It can be seen, that the best result in this case coincides with the best result obtained when the Pessimistic strategy is applied.

In order to compare the implemented optimization strategies: *Optimistic and Pessimistic/Bracketing approaches*, the absolute errors are calculated for the best chosen compromise solutions by:

$$\delta_{aj} = | q_{j,opt}(x) - q_j^*(x) | \quad (8)$$

where $q_j^*(x)$ is the best value from all Pareto-optimal solutions for the *j-th* quality characteristic, coinciding with the reference point of the optimistic approach. The relative error in this case can be calculated by:

$$\delta_{rj} = \frac{\delta_{aj}}{\Delta_j} * 100\% \quad (9)$$

The calculated results are presented in Table 10.

From Table 10 can be seen that the comparison of obtained best working regimes of the applied multi-criteria optimization strategies give close results. The biggest compromise is done with the resist thickness loss mean $\tilde{y}_5$(p), which is between 55 % and 71 % from the region of the optimal values of obtained Pareto-optimal solutions.

## CONCLUSIONS

A robust engineering design approach was applied successfully to EBL production processes for product production design aiming testing the fulfilment of pre-set technological requirements for the produced PMMA resist profiles. In such cases the integration of product quality is realized by design.

The implementation of the robust engineering design approach involves several stages, after the determination of the product quality characteristics and the influencing system and process parameters: design of simulated experiment, performing the experiments (simulated), estimation of regression models and the tolerances for the input process parameters, estimation of models for means and the variances of the quality characteristics, multicriterial optimization. Finally, conclusions can be drawn from the obtained results: are the set tolerances enough or overestimated for obtaining the desired

product quality; what are the optimal process parameter settings, that ensure robustness toward the errors in the factors in production conditions; is the system needed to be upgraded; which process parameters are most influential for the variance of the quality characteristics; which quality characteristic is most sensible toward the process variations. Additionally, knew knowledge can be reached during such investigation process and the product design can be performed more efficiently.

The investigation made for production of PMMA resists by EBL process showed that the variances of the mean sidewall angle and the thickness loss are bigger and depend strongly on the development time. The resist thickness also influences the thickness loss after development. The variation of the PMMA resist profile can be minimized significantly by applying the robust engineering approach. If this is not enough, improvement can be obtained by reduction of the tolerance limits of the process parameters, which is unwanted and costly solution.

***Acknowledgements***

*The research was supported by the Bulgarian National Science Fund under project KP-06-N27/18.*

**REFERENCES**

1. I. Vuchkov, L. Boyadjieva, Quality Improvement with Design of Experiments. A Response Surface Approach, Kluwer, Dordrecht, 2001.
2. E. Koleva, I. Vuchkov, Model-based approach for quality improvement of EBW applications in mass production, Vacuum, 77, 2015, 423-428.
3. G.M. Mladenov, E.G. Koleva, K.Zh. Vutova, in: M.R. Nemtanu, M. Brasoveanu (Eds.), Electron lithograpy of submicron- and nano-structures, Practical Aspects and Applications of Electron Beam Irradiation Transworld Research Network, India, 2011, 135-166.
4. I. Kostic, K. Vutova, E. Koleva, R. Andok, A. Bencurova, A. Konecnikova, G. Mladenov, in: A. Méndez-Vilas, A. Solano-Martín (Eds.), Polymer science: research advances, practical applications and educational aspects: Study on polymers with implementation in electron beam lithography, Formatex Research Center, 2016, 488-497.
5. K. Vutova, G. Mladenov, Sensitivity, contrast and development process in electron and ion lithography, Microelectronic Eng., 57-58, 2001, 349-353.
6. G. Mladenov, Electron and Ion Technologies, Publ. Prof. Marin Drinov, 2009.
7. K. Vutova, E. Koleva, G. Mladenov, in: M. Wang (Ed.), Chapter 18 Computer Simulation of Processes at Electron and Ion Beam Lithography, part 2: Simulation of resist developed images at Electron and Ion Beam Lithography, Lithography, INTEH Publ. Hause, Vukovar, Croatia, Printed in India, 2010, 351-378.
8. A. Rosenbush, Z. Cui, E. DiFabricio, M. Gentili, N. Glezos, G. Meneghini, B. Nowotny, G. Patsis, P. Prewett, I. Raptis, Simulation of chemically amplified resist processes for 150 nm e-beam lithography, Microelectron. Eng., 46, 1999, 379-382.
9. M. Parikh, Electron Physics in Device Microfabrication. II Electron Resists, X-Ray Lithography, and Electron Beam Lithography Update, J. Appl. Phys., 50, 6, 1979, 4371-4377.
10. QstatLab home page: http://www.qstatlab.co.uk/eng/index.html
11. S. Stoyanov, Analyses of Methods and Algorithms for Modelling and Optimization of Biotechnological Processes, Bioautomation, 13, 2, 2009, 1-18.